Shear stress induced KLF4 is a key determinant in AVM pathogenesis

Kuheli Banerjee[1*], Johannes Gahn[1*], Yanzhu Lin[1*], Xinhao Lei[1], Purnima Gupta[1], Mariona Graupera[2], Martin Schwartz[3], Roxana Ola[1#]

[1]Experimental Pharmacology Mannheim (EPM), European Center for Angioscience (ECAS), Medical Faculty Mannheim, Heidelberg University, Germany
[2]Josep Carreras Leukaemia Research Institute (IJC), Badalona, Spain
[3]Yale Cardiovascular Research Center, Yale School of Medicine, New Haven, CT, USA

[*] equal contribution

#corresponding author

Abstract

Background: Vascular networks form, remodel and mature under the influence of both fluid shear stress (FSS) and soluble factors. For example, FSS synergizes with Bone Morphogenic Protein 9 (BMP9) and BMP10 to promote vascular stability. Mutation of the BMP receptors ALK1 and Endoglin or the downstream effector SMAD4 leads to Hereditary Hemorrhagic Telangiectasia (HHT), characterized by fragile and leaky arterial-venous malformations (AVMs). But how endothelial cells (ECs) integrate FSS and BMP signals in normal vascular development and homeostasis, and how mutations give rise to malformations is not well understood.

Results: Here we show that loss of *Smad4* in the murine ECs leads in the one hand to increased sensitivity to flow and the resulting AVMs are characterized by excessive elongation and polarity against the flow and in the other hand, blocks the anti-proliferative effects of high FSS. Cellularly, we identified increased proliferation-mediated loss of arterial identity as the main event triggering AVM formation in *Smad4* depleted ECs. Molecularly, we found that flow-induced excessive KLF4-PI3K/AKT-CDK6 pathway activation mediates the enhancement in morphological responses to flow triggering AVMs.

Conclusions: Our study showed that loss of polarization against the flow is not required for AVM formation in SMAD4 ECko. Instead, increased EC proliferation and loss of arterial identity due to PI3K/Akt-Cdk6 hyperactivation and Klf4 over-expression are the main events associated with AVM formation.

Introduction

Vascular networks form, remodel and mature under the influence of multiple mechanical and biochemical signals, but how these are integrated to promote vascular development and adult homeostasis is not well understood. Fluid shear stress (FSS) from blood flow is a critical variable that determines vascular endothelial cell (EC) number, shape and movement in vascular development and maintenance[1]. One aspect of EC flow responses is the existence of a cell-autonomous shear stress set-point specific to each vessel type. FSS near the set-point promotes EC elongation and alignment parallel to the flow, and stabilizes the vessel whereas flow that is persistently above or below this level triggers vessel remodeling to restore FSS to the appropriate magnitude[2]. ECs also polarize and migrate according to the flow direction; in different systems this may be with or against the flow[3], but in the developing retina is against the flow, which is proposed to be important in guiding vessel formation[4].

We previously found that shear stress within the physiological range synergizes with secreted Bone Morphogenic Protein (BMP) 9 and BMP10 to activate Smad 1/5, which promotes EC quiescence and vascular homeostasis. This pathway contributes to the inhibition of EC proliferation by FSS and to expression of factors that mediate pericyte recruitment, thus, stabilizing the vessels[5]. By contrast, FSS activates the related Smad2,3 pathway only at low FSS magnitude to induce inward arterial remodeling[6].

Consistent with its role in vascular homeostasis, depletion in the canonical BMP9/10 signaling components in neonatal murine EC results in dilated, leaky arterial-venous malformations (AVMs) in regions of high flow[5,7,8]. These vascular lesions are a characteristic of the vascular disorder Hereditary Hemorrhagic Telangiectasia (HHT), an autosomal dominant condition caused by loss-of-function (LOF) heterozygous mutations in the BMP9/10 receptors Activin Like Kinase 1 (*ALK1*), linked to HHT2, the auxiliary co-receptor- *ENG*, linked to HHT1, and the transcriptional effector- *SMAD4*, linked to Juvenile Polyposis JP-HHT[9-11].

These findings suggest that the canonical BMP9/10-Smad signaling plays a crucial role in shear stress regulation of vascular homeostasis and that AVMs arise from disruption of these mechanisms. One important mediator downstream of this pathway is PI3K/AKT, which is hyperactivated in HHT lesions in human patients and in mouse models[8,12,13]. Pharmacological inhibition of PI3K or depletion of EC *Akt1* rescued AVM formation in HHT murine models[8,13].

Interestingly, PI3K/AKT is activated in ECs by FSS downstream of the PECAM1-VE-cadherin-VEGFRs mechanosensory receptor complex[14], thus, is also connected to flow signaling.

These principles were established via study of *ALK* and *ENG* mutations but have not been closely examined in the context of SMAD4 mutation/JP-HHT. We therefore set out to establish the role of Smad4 in EC flow signaling and AVM formation.

Results

Smad4 signaling maintains the shear stress set-point-mediated EC responses

Impaired responses of EC to FSS including migration direction, proliferation and changes in EC size and cell fate have proposed to mediate HHT lesions, mainly in models of HHT1 and HHT2, ie., mutations in *ENG* and *ALK1*[7,15]. To explore flow-mediated EC events in JP-HHT, where *SMAD4* is mutated, we depleted primary human umbilical cord ECs (HUVECs) for *SMAD4* using small interfering RNA (siRNA) vs *CTRL* siRNA (confirmed in **Figure 1G**). Cells were subject to laminar shear stress at 1 or 12 DYNES/cm^2 for 24 and 48 hours (**Figure 1A-I**). *SMAD4* depleted HUVECs were more elongated without flow (0 hours) (**Figure 1A,D**). At 24h under 12 DYNES/cm2, cells elongated further and aligned better in the direction of flow compared to controls (**Figure 1B,E;** quantified in **H,I).** Under 1 DYNE/cm^2 stress, *CTRL* HUVECs failed to elongate or align even at 48 hours, whereas *SMAD4* depleted HUVECs showed distinct elongation and alignment over this time (**Figure 1C,F,I**). EC responses to flow are thus, both faster and more sensitive after SMAD4 knock down.

To test these observations *in vivo*, we measured the ratio length/width of individual EC labelled for VE cadherin and ERG within the capillaries in *Cdh5-Cre* negative (*Smad4* Fl/Fl-control) versus AVMs in tamoxifen inducible *Smad4* EC specific deficient postnatal day 6 (P6) (*Smad4*$^{i\Delta EC}$) retinas. These measurements confirm increased morphological EC responses to flow upon *Smad4* depletion (**Figure 1J,K,L**). Together, these results imply that SMAD4 signaling restricts shear stress-mediated EC shape responses to flow.

ECs in the postnatal retina polarize and migrate against the flow direction, from the veins towards the arteries, with the degree of polarization correlating with shear stress magnitude[4]. Disrupted polarization and impaired movement of ECs against the direction of flow has been proposed to mediate AVM formation in *Eng* and *Alk1* mutants[7,15]. We therefore analyzed polarity in capillaries and AVMs in *Smad4 Fl/Fl* and *Smad4*$^{i\Delta EC}$ P6 retinas by staining for Golph4 to label the Golgi apparatus, Erg for the EC nuclei and Isolectin B4 (IB4) to visualize the endothelium (**Figure 1M,N**). The relative position of the Golgi and nuclei were then quantified (**Figure 1O**). EC polarization against the predicted flow direction was moderately increased in *Smad4*$^{i\Delta EC}$ (**Figure 1M,N,O**). Thus, multiple EC morphological responses to shear stress are increased after SMAD4 KO *in vitro* or Smad4 ECko *in vivo*.

It well established that physiological high FSS inhibits EC proliferation[16]. As expected[8], labelling of *Smad4 Fl/Fl* and *Smad4*$^{i\Delta EC}$ retinas for the mitotic marker KI67 and the total EC marker IB4 revealed increased EC proliferation in AVMs (**Figure 1Q,P,R**). *In vitro*, EdU labeling to identify cells in S phase showed that *SMAD4* depletion increased baseline cell cycle progression and completely blocked the inhibition by high shear stress (**Figure 1S**). Thus, Smad4 is required for flow-mediated repression of EC proliferation. Taken together, these results show that Smad4 resembles Alk1 and Eng in that it is also required for flow-induced quiescence but is opposite in that it suppresses rather than enhances morphological responses to flow.

Smad4 depletion induced PI3K/AKT activation regulates flow-mediated EC responses

We previously identified an increased in PI3K/AKT activity upon inactivation of BMP9/10-Alk1-Smad4 in ECs, which was further augmented by high FSS[8,13]. To further understand if increased responsiveness of *SMAD4* deficient cells to FSS is due to PI3K/AKT pathway activation, we subjected *CTRL* siRNA versus *SMAD4* depleted HUVECs to increasing magnitudes of shear stress (1-5-12 DYNES/cm^2). *SMAD4* deletion significantly increased AKT phosphorylation at serine 473, a marker of activation, under static condition and increasing flow magnitudes had an additive effect (**Figure 2A,B**). To assess the role of activated AKT in the amplified response to FSS, we inhibited PI3K/AKT signaling for 48 hours using a specific PI3K inhibitor- Pictilisib (confirmed by Western Blot (WB)) (**Figure 2C,D**) or by transfection with *AKT1* siRNA (**Figure 2E-H**). Inhibition of PI3K-AKT signaling by either method significantly rescued the length/width ratio in *SMAD4* depleted HUVECs without affecting EC alignment (**Figure 2E-H**).

To test *in vivo*, we treated *Smad4 Fl/Fl* and *Smad4*$^{i\Delta EC}$ pups with Pictilisib and examined retinas labeled with IB4, Erg and Golph4. Here, we found that PI3K inhibition blunted the axial polarity in both *Smad4 Fl/Fl* and *Smad4*$^{i\Delta EC}$ retinas (**Figure 2 I,J,K**). EdU labeling in these mice showed that inhibition of AKT rescued the excessive EC proliferation in *Smad4*$^{i\Delta EC}$ vascular plexus ECs (**Figure 2L**). *In vitro*, inhibition of PI3K also reversed the excess cell cycle progression after SMAD4 depletion in ECs under high FSS (**Figure 2M**). Thus, endothelial SMAD4 functions to restrain flow-induced PI3K/AKT and downstream responses including elongation, polarization against the flow and proliferation but not the EC alingment.

High flow-induced KLF4 is a key determinant in AVM formation

Within the retinal developing plexus, the shear stress levels are the highest in the vascular plexus close to the optic nerve, and gradually decreasing toward the sprouting front[17,18]. To gain insights into Smad4 regulation in this context, we labelled *Smad4* Fl/Fl and *Smad4*$^{i\Delta EC}$ retinas for Krüppel like transcription factor (Klf4), a gene that shows strong, dose-dependent induction by FSS [19], and for IB4 (**Figure 3A-D'**). In control, *Smad4* Fl/Fl retinas, Klf4 expression was minimal in the low shear vascular front and capillary ECs (**Figure 3A**), moderate in higher flow large veins, increased further in larger arteries, and at the highest intensity at the first retinal branch points where the wall shear stress is maximal (**arrows in Figure 3B,B'**). This specific region corresponds to the location where the AVMs most often form[8]. In *Smad4*$^{i\Delta EC}$ retinas, *Klf4* expression was highly upregulated in AVMs at the highest intensity relative to the feeding artery and vein (**arrows in Figure 3D and Figure3D',E**). The arteries and veins upstream of AVMs (**yellow arrows in Figure 3D,D'**) or vessels not engaged in AVMs (**white arrows in Figure 3D,D'**) showed lower Klf4 intensity. This result is consistent with recent findings showing lower flow outside of AVMs in embryos with decreased Cx37[20]. It also suggests that FSS-induced *Klf4* expression may be partially restrained by Smad4. To address this question in a well controlled system, we subjected *CTRL* versus *SMAD4* depleted HUVECs to increasing magnitudes of laminar FSS (1-5-12 DYNES/cm^2). Smad4 depletion moderately enhanced flow-induced *KLF4* induction (**Figure 3F**). These results suggest that high Klf4 within AVM ECs is likely a consequence of both increased sensitivity and high FSS.

Previous studies have shown that high expression of Klf2, a close homolog of Klf4 induces EC elongation[21]. We therefore considered its role in the altered behaviours of Smad4 ECko or knockdown cells. To test its function *in vivo*, we generated two genetic models. First, we examined EC specific Tx-inducible *Klf4* LOF neonates (*Klf4*$^{i\Delta EC}$) where AVMs were induced by administration of blocking antibodies (blAb) for BMP9/10 (**Figure 3G,H**) and secondly, we created EC specific Tx-inducible double ko mice, *Smad4;Klf4*$^{i\Delta EC}$ (**Figure 3I,J**). Tx was injected at P1-P3 and retinas were analysed at P6. Efficient *Smad4* and *Klf4* gene deletion was validated by qPCR from P6 mouse lung endothelial cells (mLECs; **Figure 3K**). Blockade of BMP9/10 in control *Klf4 Fl/Fl* retinas led to formation of AVMs (average of 3.6-4 AVMs per retina) and an increase in vascular front density similar to Smad4 ECko (**Figure 3G,I,L,M**). *Klf4* inactivation rescued AVM formation in both models but not the excessive sprouting at the vascular front

(**Figure 3H,J,L,M**). Thus, shear stress-induced Klf4 is a key determinant in AVM pathogenesis and the first molecular marker identified to-date to discern flow-dependent AVM formation from flow-independent excessive sprouting.

KLF4 mediates flow-induced hyper-responsiveness of *SMAD4* depleted HUVECs

To address mechanisms, we next investigated which of the aberrant EC flow responses require KLF4. HUVECs depleted for either *SMAD4* or *KLF4* or both, *SMAD4;KLF4* using the siRNA strategy were grown without flow and with low or high flow for 48 hours (**Figure 4A-C**). *KLF4* inactivation rescued the elongated morphology of *SMAD4* depleted HUVECs under all conditions and had no effect on cell alignment under flow (**Figure 4B-G**).

Conversely, we overexpressed *KLF4* using a lentiviral vector in HUVECs (*KLF4 OE*; confirmed in **Figure 4J,K**) and subjected cells to low FSS for 48 hours (**Figure 4H-N**). *KLF4* OE increased cell elongation under static conditions (**Figure 4H,L**), which was enhanced by low FSS (**Figure 4I,L**). *KLF4* OE cells also aligned better in the flow direction (**Figure 4I,M**). Measurement of EdU incorporation showed that KLF4 increased cell cycle progression at baseline and reduced the anti-proliferative effect of flow (**Figure 4N**). Klf4 OE thus induces many of the key effects of Smad4 deletion. Together, these results show that Klf4 contributes to the morphological effects mediated by Smad4 LOF.

KLF4 mediates the shear stress induced aberrant behaviours in AVMs

To address EC Golgi orientation, *Fl/Fl*, *Smad4*$^{i\Delta EC}$, *Klf4*$^{i\Delta EC}$ and *Smad4*;*Klf4*$^{i\Delta EC}$ retinas were examined. Compared to *Fl/Fl* mice, *Klf4* deficient capillaries showed reduced polarization against the flow direction; in *Smad4*$^{i\Delta EC}$ retinas, additional *Klf4* inactivation blunted the increased axial polarity (**Figure 5A-C**). *Klf4* ko ECs were less elongated than *Fl/Fl* ECs and *Klf4* inactivation rescued the excessive elongation of *Smad4*$^{i\Delta EC}$ ECs, thus confirming our *in vitro* findings (**Figure 5D**). To assay Klf4-mediated EC cell cycle progression, we injected EdU into Tx induced non-CDH5 *Fl/Fl*, S*mad4*$^{i\Delta EC}$ and S*mad4*;*Klf4*$^{i\Delta EC}$ P6 pups, 4 hours before labeling the retinas for EdU and ERG (**Figure 5E**). As previously observed, ERG+/EdU+ double positive ECs increased markedly in *Smad4*$^{i\Delta EC}$ retinas, exclusively in AVMs. *Klf4* inactivation significantly decreased the number of ERG/+EdU+ in the vascular plexus of *Smad4*$^{i\Delta EC}$ retinas to comparable

levels to *Fl/Fl* retinas (**Figure 5E,F).** Elevated Klf4 thus contributes to increased polarity and proliferation in Smad4 ECko blood vessels.

Flow induced KLF4 acts upstream of mechanosensory complex-PI3K/AKT pathway

To untangle the relationships between KLF4 and PI3K, we inhibited PI3K/AKT with Pictilisib and subjected HUVECs to 5 DYNES/cm^2 for 2 hours. RT-PCR results show no effect of Pictilisib on *KLF4* under any of these conditions (**Figure 6A**). We also considered the role of the junctional mechanosensory receptor complex that mediates flow responses including PI3K activation[22,23]. Depletion of each of the components of the mechanosensory receptor complex had no effect on the flow upregulation of *KLF4* expression (**Figure 6B**). Thus, *KLF4* expression does not require PI3K or the mechanosensory junctional receptor complex.

We then tested effects of *KLF4* on AKT activation, with and without flow and *SMAD4* knockdown. *KLF4* inactivation led to a decrease in pAKT in static conditions, blunted the increase in Akt activity under flow and rescued AKT hyperactivation in *SMAD4* depleted HUVECs, in both static and flow conditions (**Figure 6C,D**). To further test if flow-induced KLF4 is upstream of PI3K we examined the *KLF4* OE HUVECs. KLF4 upregulation was sufficient to activate AKT, with or without FSS (**Figure 6E,F**). To test these findings *in vivo,* we labelled retinas for phosphorylated S6 ribosomal protein (pS6), a downstream target of AKT activation, as well as IB4. *Smad4*$^{i\Delta EC}$ retinas showed high pS6 as expected, which was largely rescued by *Klf4* deficiency (**Figure 6G-I**). KLF4 is thus upstream of PI3K to control EC elongation and proliferation after Smad4 ECko.

Increased EC proliferation triggers AVM formation in *Smad4* deficient AVMs

Current models propose that decreased polarization and migration of ECs against the direction of flow is critical in AVM formation upon *Eng* and *Alk1* ECko. The current data show that AVM formation upon *Smad4* depletion involves, if anything, improved polarity. These findings prompted us to investigate if increased EC proliferation is the main event driving AVMs. Performing cell cycle distribution in ECs FACS sorted from *Smad4 Fl/Fl* versus *Smad4*$^{i\Delta EC}$ retinas, we revealed an increase in actively cycling ECs in S/G2/M together with a decrease in ECs in G1, confirming increased EC proliferation upon *Smad4* depletion (**Figure 7A**).

Cell cycle progression is tightly regulated by members of the cyclin dependent kinase (CDK) family. To identify dysregulated cell cycle regulators upon *SMAD4* LOF, we performed WB

analysis to multiple cell cycle regulators. We observed increased phosphorylation of Retinoblastoma (RB) and expression of E2F1 transcription factor after *Smad4* depletion, together with an elevated CDK2 and CDK6 protein levels (**Figure 7B**). *KLF4* inactivation alone led to reduced levels in all the main cell cycle regulators, suggesting cell cycle arrest. *KLF4* inactivation in *SMAD4* LOF HUVECs normalized levels of pRB1, E2F1, CDK2 and CDK6 (**Figure 7B**).

To test whether effects on cell cycle are the main drivers of AVMs, we treated *Smad4 Fl/Fl* and *Smad4*$^{i\Delta EC}$ pups with Palbociclib, a specific inhibitor of CDK4/6 shown to efficiently inactivate RB and block cell cycle progression[24] (**Figure 7C**). As expected, labeling retinas for KI67 and IB4 showed decreased EC proliferation (**Figure 7D)** and significant rescue of AVMs (**Figure 7E**). Taken together, these results suggest that increased cell proliferation as a result of flow-induced excessive KLF4-AKT-CDK4/6 drives AVM formation.

Recent data show that cell cycle arrest is a prerequisite for maintaining arterial identity[24]. Conversely, dysregulated BMP9-SMAD4 signaling leads and to loss of arterial and gain of venous identity[8,13,25].

To further assess the connection between cell cycle and arterial identity, we analyzed HUVECs depleted for *KLF4* and *AKT,* or treated with Palbociclib to inhibit cell cycle progression. RT-PCR identified a significant increase in expression of the arterial markers *EPHRINB2* and *SOX17* upon inhibition of KLF4-AKT-CDK4/6 pathway (**Figure 7F,G**).

To test these results *in vivo*, we labeled retinas for Sox17 (**Figure 7H**). In *Fl/Fl* retinas, Sox17 was confined to ECs in main arteries and a few arterioli. In AVMs in *Smad4*-deficient retinas, Sox17 expression was completely abrogated. In *Klf4* ECko retinas, Sox17 expression expanded towards the vein and capillary ECs. *Klf4* inactivation in *Smad4*$^{i\Delta EC}$ retinas largely rescued *Sox17* expression in arteries. CDK4/6 inhibition led to even greater expansion of Sox17 expression in capillary and venous ECs and restored Sox17 expression in Smad4 ECko arteries (**Figure 7H).** Collectively, these results suggest that increased EC proliferation-mediated loss of arterial identity is the main cell event triggering AVM formation**.**

Figure legends

Figure 1. SMAD4 signaling maintains the FSS set-point to restrict flow mediated EC responses. (**A-F**) Negative images of VE Cadherin staining of HUVECs transfected with *CTRL* (**A-C**) and *SMAD4* (**D-F**) *siRNAs* grown in static (**A**,**D**) or increasing flow magnitudes: 12 DYNES/cm^2 (**B**,**E**) or 1 DYNE/cm^2 (**C**,**F**) for 24 hours and 48 hours, respectively. The direction of the flow is right to left. (**G**) *SMAD4* qPCR expression (fold change) in HUVECs treated with *CTRL* versus *SMAD4* siRNAs. (**H**,**I**) Quantification of length/width ratio and of EC alignment parallel to flow direction (%) in *CTRL* and *SMAD4* siRNAs HUVECs grown in static versus subjected to 12 DYNES/cm^2 (**H**) and 1 DYNE/cm^2 (**I**). (**J**,**K**) Labeling of postnatal day 6 (P6) Tx induced *Smad4 Fl/Fl* (**J**) and *Smad4*$^{i\Delta EC}$ (**K**) retinas for Erg (labelling the EC nuclei-white), and VE-Cadherin (green). (**L**) Quantification of length/width ratio in capillaries versus AVMs in *Smad4 Fl/Fl* and *Smad4*$^{i\Delta EC}$ retinas. (**M**,**N**) Labeling of postnatal day 6 (P6) Tamoxifen (Tx) induced *Smad4 Fl/Fl* and *Smad4*$^{i\Delta EC}$ retinas for Erg (labelling the EC nuclei-white), Golph4 (labeling the Golgi-red) and Isolectin (IB4) (labeling vessels-green). (**O**) Quantification of EC polarization against versus towards versus non-oriented (neutral) in the capillaries of *Smad4 Fl/Fl* and *Smad4*$^{i\Delta EC}$ retinas. (**Q**,**P**) Labeling for KI67 (white) and IB4 (green) of the vascular plexus from P6 *Smad4 Fl/Fl* (**Q**) and *Smad4*$^{i\Delta EC}$ (**P**) retinas. (**R**) Quantification of the number of KI67 positive nuclei per vascular area in the vascular plexus (%). (**S**) EC proliferation in response to 12 dynes/cm^2 for 24 h after transfection with *CTRL* or *SMAD4* siRNA. Cell proliferation was measured by incorporation of EdU during the 4 hours. Scale Bars: 100μm in **A-F** and **M**,**N**, **200**μm in **J**,**K** and 50μm in **Q**,**P**. Red arrows in **N** point to the direction of polarization against the flow. Yellow arrows in **Q**,**P** point to KI67+ ECs in the vascular plexus. **a**: artery, **v**: vein. Error bars: s.e.m., *P<0.05,**P<0.01,***P<0.001, ns- non-significant student T test.

Figure 2. Smad4 induced PI3K/AKT activation regulates flow-mediated EC responses

Western Blot (WB) analysis of HUVECs transfected with *CTRL* or *SMAD4* siRNA grown in static or subjected to increasing magnitudes of shear stress: 1-5-12 DYNES/cm^2 for 4 hours. (**B**) Quantifications of pAKT levels normalized to total AKT. (**C**) WB analysis of HUVECs grown in static versus subjected to 5 DYNES/cm^2 treated with PBS or Pictilisib (PI3Ki-75nM) for 4 hours.

(**D**) Quantifications of pAKT levels normalized to total AKT. (**E**,**F**) Negative images of VE-CADHERIN staining of HUVECs transfected with *CTRL* and *SMAD4 siRNAs* subjected to 12 DYNE/cm^2 and treated with PI3K inhibitor or with *AKT1* siRNA for 48 hours. (**G**,**H**) Quantification of the length/width ratio (**G**) and of EC alignment parallel to flow direction (%) (**H**). (**I**,**J**) Confocal images of retinas from P6 *Fl/Fl* (**I**) and *Smad4*$^{i\Delta EC}$ (**J**) from pups treated with PBS or PI3K inhibitor labeled for Erg (white) and Golph4 (Golgi-red) and IB4 (green). Yellow arrows in **J** mark the AVMs. (**K**) Quantification of EC polarization: against the direction of flow, towards the direction of flow and non-oriented (neutral) in capillaries and AVMs from P6 retinas of *Smad4Fl/Fl* and *Smad4*$^{i\Delta EC}$ pups treated with PBS or PI3Ki. (**L**) Quantification of EdU+/Erg+ ECs in the vascular plexus of *Smad4*$^{i\Delta EC}$ retinas in PBS versus PI3Ki treated pups (**M**) EC proliferation (incorporation of EdU) in response to 12 DYNES/cm^2 for 24 hours after transfection with *CTRL* or *SMAD4* siRNA in PBS versus PI3ki (Pictilisib) treatment.

Scale Bars: 100μm in **E**,**F**,**I**,**J**. **a**: artery, **v**: vein. Error bars: s.e.m., **P*<0.05,***P*<0.01,****P*<0.001, ns- non-significant, student T test.

Figure 3. High Flow-induced KLF4 is a key determinant in AVM formation

(**A-D'**) Labeling of Tamoxifen (Tx) induced *Smad4* Fl/Fl and *Smad4*$^{i\Delta EC}$ retinas for Klf4 (green) and IB4 (white) in the sprouting front (**A**,**C**) versus vascular plexus (**B**,**B'** and **D,D'**). Small red/blue arrowheads in **B**,**B'** indicate the first branch points in artery/vein. Big red arrowheads in **D**,**D'** indicate increased KLF4 intensity within the AVM. Small yellow/white arrowheads indicate vessels upstream of AVMs or vessels not engaged in AVMs expressing very low KLF4. (**E**) Quantification of KLF4 pixel intensity/EC in arteries, capillaries and veins in Fl/Fl capillaries and *Smad4*$^{i\Delta EC}$ AVMs. **(F)** *KLF4* mRNA expression by qPCR in HUVECs transfected with *CTRL* and *SMAD4* siRNAs grown in static or subjected to increasing magnitudes of shear stress: 1-5-12 DYNES/cm^2 for 2 hours. (**G**,**H**,**I**,**J**) Staining of P6 retinas with IB4 of *Klf4 Fl/Fl* (**G**) and *Klf4*$^{i\Delta EC}$ (**H**) treated with blocking antibodies for BMP9/10 (BMP9/10blAb) and of *Smad4*$^{i\Delta EC}$ (**I**) and double knockout mice:*Smad4;Klf4*$^{i\Delta EC}$(**J**). Red arrows in **G, I** and **J** mark the AVMs. (**K**) *Smad4* and *Klf4* mRNA expression by qPCR in purified mouse lung endothelial cells (mLECs) isolated from P6 Tx injected mice. (**L**) Quantification of P6 retinal AVMs' number. (**M**) Quantification of vascular density at the retinal front (%).

Scale Bars: 100μm in **A**-D' and 20μm in **G**,**H**,**I**,**J**. Error bars: ***P*<0.01, ****P*<0.001, ns- non-significant, student T test.**a**: artery, **v**: vein.

Figure 4. KLF4 mediates the hyper-responsiveness of *SMAD4* depleted cells upon flow

(**A**-**C**) Negative images of VE CADHERIN staining of HUVECs transfected with *CTRL*, *SMAD4, KLF4* and *SMAD4;KLF4* siRNAs grown in static (**A**) or subjected to 1 DYNE/cm^2 (**B**) and 12 DYNES/cm^2 (**C**) for 48 hours. (**D**-**G**) Quantification of the length/width ratio and of EC alignment parallel to the flow direction (%) of HUVECs transfected with *CTRL*, *SMAD4, KLF4* and *SMAD4;KLF4siRNAs* grown in static or subjected to 1 DYNE/cm^2 (**D**,**E**) and 12 DYNES/cm^2 (**F**,**G**). (**H**,**I**) Negative images of VE CADHERIN staining of HUVECs transfected with *CTRL-OE* and *KLF4-OE* constructs grown in static (**H**) or subjected to 1DYNE/cm^2 for 48 hours (**I**). (**J**) WB analysis of HUVECs transfected with an empty lentiviral construct (*CTRL-OE*) and an overexpression lentivirus for *KLF4* (*KLF4-OE*). (**K**) Quantification of KLF4 protein expression levels normalized to GAPDH. (**L**,**M**) Quantification of the length/width ratio (**L**) and of EC alignment (%) parallel to the flow (**M**) of *CTRL-OE* and *KLF4-OE* HUVECs grown in static versus 1 DYNE/cm^2 conditions for 48 hours. Scale Bars: 100μm in **A**-**C** and **H**,**I**. Error bars: s.e.m., n.s- non-significant, **P*<0.05, ***P*<0.01, ****P*<0.001, student T test.

Figure 5. KLF4 mediates the shear stress induced aberrant behaviour in AVMs

(**A**) Confocal images of P6 Tx induced *Fl/Fl*, *Smad4*$^{i\Delta EC}$, *Klf4*$^{i\Delta EC}$ *and Smad4;Klf4*$^{i\Delta EC}$ retinal plexus labeled for Erg (white), Golph4 (Golgi-red) and IB4 (green). (**B**) Panels illustrating EC polarization based on position of Golgi versus nucleus in the direction of migration (green arrows). (**C**) Quantification of EC polarization: against the direction of flow, towards the direction of flow and neutral in capillaries from P6 Tx induced retinas from the indicated genotypes. (**D**) Quantification of length/width ratio in capillary ECs in the indicated genotypes. (**E**) Labeling for EdU (white) and Erg (green) in vascular plexus of retinas from P6 *Fl/Fl*, *Smad4*$^{i\Delta EC}$ and *Smad4;Klf4*$^{i\Delta EC}$ P6 mice. Red arrowheads indicate the ERG/EdU+ cells in the AVMs. (**F**) Quantification of the number of ERG/EdU double + EC nuclei in the vascular plexus (%). Scale Bars: 100μm in **A**,**B**,**E**. Error bars: n.s- non-significant, **P*<0.05, ***P*<0.01, ****P*<0.01, student T test. **a**: artery, **v**: vein.

Figure 6. Flow-induced KLF4 acts upstream of mechanosensory complex-PI3K/AKT pathway activation

(**A**,**B**) *KLF4* mRNA expression by qPCR in HUVECs grown in static versus subjected to 5 DYNES/cm^2 treated with PBS versus Pictilisib (PI3Ki-75nM) (**A**) and in *CTRL*, *VEGFR2*, *PECAM* and *CDH5* siRNAs treated HUVECs grown in static versus 5 DYNES/cm^2 (**B**) for 2 hours. (**C**) WB analysis of HUVECs transfected with *CTRL*, *SMAD4, KLF4 and SMAD4;KLF4* siRNAs grown in static or subjected to 5 DYNES/cm^2 for 4 hours. (**D**) Quantifications of pAKT levels normalized to total AKT. (**E**) WB analysis of HUVECs transfected with an empty lentiviral construct (*CTRL-OE*) and an overexpression lentivirus for *KLF4* (*KLF4-OE*). (**F**) Quantifications of pAKT levels normalized to total AKT. (**G**) Anti-pS6 (white) alone and double labeling for pS6 and IB4 (red) staining (**H**) of retinal flat mounts from Tx induced P6 *Fl/Fl*, *Smad4*$^{i\Delta EC}$, *Klf4*$^{i\Delta EC}$ and *Smad4;Klf4*$^{i\Delta EC}$. (**I**) Quantification of the percentage of pS6+ vascular area per field of view in indicated genotypes.

Scale Bars: 100μm in **G**,**H**. Error bars: s.e.m., ns: non-significant, **P*<0.05, ***P*<0.01, ****P*<0.001, student T test.

Figure 7. EC proliferation triggers AVM formation in *Smad4* deficient AVMs

(**A**) FACS analysis to assess cell cycle distribution in ECs from *Smad4 Fl/Fl and Smad4*$^{i\Delta EC}$ P6 retinas. (**B**) WB analysis for the indicated proteins of HUVECs transfected with *CTRL*, *SMAD4, KLF4* and *SMAD4;KLF4 siRNAs*. (**C**) Confocal images of P6 Smad4 *Fl/Fl* and *Smad4*$^{i\Delta EC}$ retinas treated with DMSO or Palbociclib labeled for IB4 (white) and KI67 (green). Yellow arrows mark the KI67+ ECs within the AVMs. (**D**) Quantification of the number of KI67+ ECs per vascular area (%) in the vascular plexus. (**E**) Quantification of the number of AVMs in DMSO versus Palbociclib treated *Smad4*$^{i\Delta EC}$ retinas. (**F,G**) RT-PCR for *EPHRINB2* and *SOX17* in *CTRL*, *KLF4* and *AKT* siRNAs transfected cells and in Palbociclib treated HUVECs. (**H**) Confocal images of labeled retinas for Sox17 (white) and IB4 (red) from the indicated genotypes. Scale Bars: 100μm in **C**,**J**. Error bars: s.e.m., n.s- non-significant, **P*<0.05, ***P*<0.01, ****P*<0.001, student T test. **a**: artery, **v**: vein.

Discussion

We have revealed here that loss of Smad4 in mouse ECs triggers increased sensitivity to FSS with elevated PI3K/Akt signaling and Klf4 expression, enhanced elongation and polarization in FSS simultaneolsy with inefficient FSS-mediated cell cycle blockade and loss of arterial identity due to increased CDK2/CDK6 protein levels. It has been proposed that blood flow is 'a second hit' contributing to HHT, as murine AVMs develop in regions of high shear stress[5,8], but the mechanisms by which shear stress contributes to AVM pathology remains largely undefined. ECs display an intrinsic set-point for shear stress that determines signaling and gene expression outputs. Previous work showed that VEGFR3 expression is one factor that can determine shear stress set-point for different types of vessels[2]. Non-canonical WNT signaling was proposed to modulate axial polarity set-point to control vessel regression in low flow regions[26]. Our results identify SMAD4 signaling as a novel mechanism that "sets the set-point" for high flow-mediated EC quiescence responses: elongation, alignment and orientation. Smad4 is also critical for FSS mediated growth suppression and arterial EC fate, yet, it remains to be determined if these cell events are also linked to changes in the set point.

We previously identified an increased in PI3K/AKT signaling to be responsible for AVM formation[8,13]. Herein, we provide genetical evidence that flow-induced Klf4 further augments this pathway and contributes to AVM pathogenesis. However, the mechanism by which Klf4 regulates Akt activation requires further investigation. Interestingly, identification of this mechanism for high flow AVMs resembles molecularly other vascular malformations. The low flow venous malformations are due to increased PI3K/AKT by GOF mutations in PI3K and therefore activation of AKT[27], and similarly, GOF mutations in PI3K act as a second genetic hit in cavernous malformations, where MEKK3 activated Klf4 is the primary mechanism[28].

It is generally assumed that the mechanisms of AVM formation are similar if not identical, in HHT1, HHT2 and JP-HHT. Our data, however, argue that AVMs are not strictly identical, at least in mouse models. We found that *SMAD4* depleted cells elongate in the absence of flow and elongate further and align in response to much lower FSS. These changes presumably reflect effects on the cytoskeleton and/or cell junctions, which would be consistent with elevated PI3K[21], but remain to be defined for Klf4. In *Eng* and *Alk1* LOF mice, failure to migrate against the flow

was the main event proposed to trigger AVM formation[29,30]. Opposingly, our data suggest more migration against the flow in the AVMs upon *Smad4* ECko. Nevertheless, AVMs are characterized by gain of venous markers and contain exclusively venous like ECs. In line with a recent report emphasizing a venous origin for AVMs upon *Smad4* LOF, our observed effects on EC polarity might thus explain the enhanced migration from veins towards the arteries giving rise to AVMs[31].

These differences in flow driven migration in different mouse models may indicate either distinct cellular and molecular mechanism driving AVM formation in different mouse models, or that axial polarity/reverse migration is not important in AVM formation. As there is yet no functional evidence that migration against the flow is important in *Alk1* and *Eng* LOF AMVs*,* based on our findings, we propose instead that loss of flow-induced suppression of EC proliferation is the key cellular event triggering AVM formation upon *Smad4* depletion.

Arterial specification induced by HSS requires cell cycle arrest, a process in which Notch through Cx37- p27signaling is a key element[24]. Our results suggest that loss of *Smad4* leads to loss of arterial identity due to an increased in flow-induced excessive KLF4-PI3K/AKT-CDK6 mediated EC proliferation.

In summary, our study identified Smad4 signaling as a novel mechanism to maintain EC quiesncence by restraining flow-induced KLF4-PI3K/AKT-CDK6 activation in ECs. The mechanism by which Smad4 "sets the set-point" for FSS-mediated cel responses to maintain EC quiescence and what are the subsequent molecular events implicated, is an important direction for future studies. AVMs in HHT patients form later in life. Although our study was conducted in a developmental setting, this mechanism is likely to be important for maitenance of vascular homeostasis also n mature vessels. Thus Klf4-PI3K/Akt-CDK6 may be an attractive target for HHT patients treatment.

Acknowledgements

The authors would like to thank Dr. Gergana Dobreva and Dr. Thomas Willand (University Medical Center Mannheim) for sharing reagents and for manuscript data disscusion. We would like to thank Stefanie Uhlig, Flow Core Mannheim and Institute of Transfusion Medicine and Immunology, for excellent support.

This work was supported by grants from the Deutsche Forschungsgemeinschaft (Collaborative Research Center CRC1366 'Vascular control of organ function (Project number 39404578; AP to RO and salary to KB) and from start-up funding from Mannheim Faculty of Medicine. YL and XL were supported by China Scholarship Council no. 202006380050 and 202106200015, respectively.

Competing Interest Statement

The authors have declared no competing interest

Methods

Animal Experiments

Deletion of endothelial *Smad4* (*Smad4*$^{i\Delta EC}$) *or Klf4* (*Klf4*$^{i\Delta EC}$) was achieved by crossing *Smad4 Fl/Fl* or *Klf4 Fl/Fl* with Tx inducible *Cdh5-Cre*^{ERT2} mice. To obtain *Smad4;Klf4*$^{i\Delta EC}$ double knockout mice, we crossed *Smad4*$^{i\Delta EC}$ with *Klf4*$^{fl/fl}$ mice. Gene deletion was achieved by intra-gastric injections of 100µg Tx (Sigma, T5648) into *Smad4*$^{i\Delta EC}$, *Klf4*$^{i\Delta EC}$ and *Smad4*$^{i\Delta EC}$*;Klf4*$^{i\Delta EC}$ at postnatal days (P1-P3). Tx-injected Cre-negative littermates (*Fl/Fl*) were used as controls. The PI3K inhibitor Pictilisib (Selleckchem, S1065, 20 mg/kg/day) and CDK4/6 inhibitor Palbociclib (Selleckchem, S1116, 70 mg/kg/day) were administered intraperitoneally (i.p) at P4 and P5.

Mice were maintained under standard specific pathogen-free conditions, and animal procedures were approved by the animal welfare commission of the Regierungspräsidium Karlsruhe (Karlsruhe, Germany).

Reagents and antibodies

For immunodetection: anti-VE Cadherin (#2500S, 1:600, Cell Signaling), anti-PECAM (#sc-32732, 1:100 Santa Cruz), Isotectin B4 (IB4, #121412, 10 µg/ml, Life Technologies), anti-GOLPH4 (#ab28049; 1:200, Abcam), anti-GM130 (#610823; 1:600 BD Bioscience), anti-ERG (#92513; 1:200; Abcam), anti-KLF4 (#AF3158, 1:200, R&D systems), anti-phospho S6 (pS6 #5364, 1:200; Cell Signaling), anti VE-CADHERIN (VE CADH, #2500, 1:500, Cell Signaling anti- phospho-histone H3 (PH3, #06570; 1:500;EMD Millipore), anti-KI67 (eFluor™660, 1:100, ThermoFisher).

For WB: anti-pAKT (#4060, 1:1,000, Cell Signalling), anti-AKT (#4060, 1:1,000, Cell Signalling), anti-SMAD4 (#38454S; 1:1000; Cell Signalling), GAPDH (#5174S 1:5000, Sigma), ACTIN (A1978, 1:1000, Sigma), pRB1 (#8516S, 1:1000, Cell signaling), RB (#9309S, 1:1000, Cell signaling), E2F1 (#3743, 1:1000, Cell signaling), CDK2 (#2546, 1:1000, Cell signaling), CDK6 (#3136, 1:1000, Cell signaling).

Appropriate secondary antibodies were fluorescently labelled (Alexa Fluor donkey anti-rabbit, #R37118, Alexa Fluor donkey anti-goat 555, #A-21432, 1:250, Thermo Fisher) or conjugated to horseradish peroxidase for WB (Anti-Rabbit #PI-1000-1, Anti-Goat #PI-9500-1 and Anti-mouse #PI-2000-1 IgG (H+L), 1:5,000, Vector Laboratories).

mLECs isolation

mLECs were isolated from collagenase I-digested lung tissue using rat anti-mouse CD31 monoclonal antibody-coated Dynabeads (11035, Invitrogen) and cultured in DMEM (Sigma) supplemented with 10% fetal bovine serum (FBS), 100U/ml penicillin, 100µg/ml streptomycin, 100µg/ml endothelial cell mitogen (Biomedical Technologies, Inc.) and 10U/ml heparin for 2 days before RNA isolation.

Quantitative real-time PCR

RNAs from HUVECs or mouse lung ECs (mLECs) were purified using RNeasy-kit (74106, Qiagen). The RNA was reverse transcribed High-Capacity cDNA Reverse Transcription Kit (4368813, Thermo Fisher) and quantitative PCR were assayed using PowerUP SYBR Green Master Mix (A25778, Thermo Fisher) with a QuantStudio 3 (Thermo Fisher) according to the manufactures protocol. The following primers were used for mLECs: Klf4 (QT00095431, Qiagen), Smad4 (QT00130585, Qiagen) and Gapdh (Forward: AGGTCGGTGTGAACGGATTTG, Reverse: TGTAGACCATGTAGTTGAGGTCA). Primers used for HUVECs: KLF4 (Forward: CCCACATGAAGCGACTTCCC, Reverse: CAGGTCCAGGAGATCGTTGAA), SMAD4 (QT00013174, Qiagen), PECAM-1 (Forward: AAGTGGAGTCCAGCCGCATATC Reverse: ATGGAGCAGGACAGGTTCAGTC), KDR (QT00069818, Qiagen), CDH5 (QT00013244, Qiagen), GAPDH (Forward: CTGGGCTACACTGAGCACC Reverse: AAGTGGTCGTTGAGGGCAATG), SOX17 (QT00204099, Qiagen), EPRINB2 (forward: TATGCAGAACTGCGATTTCCAA Reverse: TGGGTATAGTACCAGTCCTTGTC).

Immunostaining

The eyes of P6 pups were fixed in 4% PFA for 17 minutes at room temperature (rt). After several washes with PBS, dissected retinas were incubated with specific antibodies diluted in blocking buffer (1% fetal bovine serum, 3% BSA, 0.5% Triton X-100, 0.01% sodium deoxycholate, 0.02% sodium azide in PBS at pH 7.4) at 4 ^{0} C overnight. The following day, retinas were washed and incubated with IB4 together with the corresponding secondary antibody in PBLEC buffer (1 mM $CaCl_2$, 1 mM $MgCl_2$, 1 mM $MnCl_2$ and 0,25% Triton X-100 in PBS) for 1 hour at room temperature (rt) and mounted in fluorescent mounting medium (RotiMount FluorCare

#HP19.1, CarlRoth). High-resolution pictures were acquired using Zeiss LSM800 confocal microscope with Airyscan Detector and the Zeiss ZEN software. Quantification of retinal v-asculature was done using Fiji and Prism 9 software.

Cell culture, siRNA transfection, overexpression HUVECs and PI3K inhibitor treatment

Human Umbilical Vein Endothelial Cells (HUVECs) were isolated from the umbilical cords of newborn, approved by the local ethics committee (2012-388N-MA, 08/11/2018, Medical Faculty Mannheim, Heidelberg University, Germany). A 3-way valve was inserted into the vein and fixed with a zip tie to wash the vein several times until the effluent buffer was transparent or slightly pink. At that point, the vein was closed with a surgical clamp, filled with a 0.2% Collagenase/Dispase (11097113001, Sigma-Aldrich) solution and incubated at 37°C for 30-45 minutes. Post-incubation the umbilical cord was emptied into 5ml of FCS and centrifuged at 1000rpm for 5 minutes. Then the cells were re-suspended in 10ml of Endothelial Cell Growth Medium MV2 with supplemental mix (C-22022, PromoCell) and 1% Penicillin/Streptomycin (P4333, Sigma-Aldrich), platted on a 10cm dish and incubated at 37°C (with 5% CO_2, 100% humidity). Cells up to passage 4 were used for experiments. Depletion of *SMAD4*, *KLF4*, *PECAM-1*, *AKT1/2, VEGFR2, CDH5* was achieved by transfecting 25 pmol of siRNA against *SMAD4* (ON-Targetplus Human SMAD4 siRNA Smart Pool, #L-003902-00-0005)), *KLF4* (siGENOME Human KLF4 siRNA; #M-005089-03-0005), PECAM-1 (5'-GGCCCCAAUACACUUCACA-3'), AKT1/2 Stealth siRNA (Thermo Fisher, VHS40082 and VHS41339), VEGFR2 (Dharmacon/Horizon, #L-003148-00-005), CDH5 (Dharmacon/Horizon, #L-003641-00-0005) using Lipofectamine RNAiMax (Invitrogen) in 2% OPTI-MEM. Transfection efficiency was assessed by western blotting and qPCR. Experiments were performed 48-60 hours post transfection and results were compared with siRNA *CTRL* (ON-TARGETplus Non-Targeting Pool D-001810-10-05). Inhibition of PI3K was achieved by using Pictilisib (S1065, Selleckchem) in a concentration of 75nM and inhibition of CDK4/6 by using Palbociclib in concentration of 2 µM. Before experiments cells were starved for 8-10 hours in 2% FCS.

For Generation of stable AKT1 and KLF4 overexpressing cell lines the AKT1 (TRCN0000473539) and KLF4 (TRCN0000492053) overexpression plasmids were obtained from Sigma (Mission TRC3.0, Sigma Aldrich, USA). For lentivirus packing, briefly, HEK293T cells

were co-transfected with lentiviral vector and packaging plasmids (pCMV-dR8.91 and pCMV-VSV-G) using X-treme GENE 9 reagent (Sigma). Culture supernatant containing viral particles was collected 36 and 72 h after transfection and concentrated by centrifugation at 1500g for 60 min at 4°C. The pellets were resuspended in 1 mL of PBS and stored at -80°C. For virus infection, Huvecs cells were transduced with optimal volume of lentiviral virus at 50% confluence in MV2 medium and 8µg/ml Polybrene (Sigma). After 24 h, the medium containing viral particles was replaced with fresh medium and after additional 24h, the infected cells were selected with 2 µg/ml puromycin for 48 h.

Exposure of endothelial cells to increased shear stress

HUVECs transfected with siRNAs or OE-HUVECs were plated in a six-well plate and on an orbital shaker (Rotamax120, Heidolph Instruments) at 50, 150 or 250 rpm to generate laminar sheer stress of 1, 5 or 12 DYNES/cm^2 respectively. Results were confirmed in a µ-Slide VI$^{0.4}$ (Ibidi, 80601) using a pump system (Ibidi, 10902).

Western blotting

HUVECs were washed with PBS and lysed with Laemmli buffer (1610740, Biorad). Samples were separated on 10% SDS-PAGE gels and transferred on 0.2µm nitrocellulose membranes (10600004, GE Healthcare). Western blots were developed with the Clarity Western ECL Substrate (1705061, Biorad) on a Luminescent image Analyzer, Fusion FX (Vilber). Bands' intensity were quantified using ImageJ.

Proliferation Assay

Proliferation analysis was performed using Click-iT EdU Alexa Fluor 488 Imaging kit (Life Technologies). P6 pups were injected with 200 µg of EdU (5 mg/mL) and sacrificed 4 hours later. EdU staining was done according the manufacturer's protocol.

Statistical analysis

All data are shown as mean ± standard error of the mean (SEM). Samples with equal variances were tested using Mann–Whitney U test or two-tailed Student's t-test between groups. P value <0.05 was considered to be statistically significant. Statistical analyses were performed for all quantitative data using Prism 9.0 (Graph Pad).

References

1 Baeyens, N., Bandyopadhyay, C., Coon, B. G., Yun, S. & Schwartz, M. A. Endothelial fluid shear stress sensing in vascular health and disease. *J Clin Invest* **126**, 821-828, doi:10.1172/JCI83083 (2016).

2 Baeyens, N. *et al.* Vascular remodeling is governed by a VEGFR3-dependent fluid shear stress set point. *Elife* **4**, doi:ARTN e0464510.7554/eLife.04645 (2015).

3 McCue, S. *et al.* Shear stress regulates forward and reverse planar cell polarity of vascular endothelium in vivo and in vitro. *Circ Res* **98**, 939-946, doi:10.1161/01.RES.0000216595.15868.55 (2006).

4 Franco, C. A. *et al.* Correction: dynamic endothelial cell rearrangements drive developmental vessel regression. *PLoS Biol* **13**, e1002163, doi:10.1371/journal.pbio.1002163 (2015).

5 Baeyens, N. *et al.* Defective fluid shear stress mechanotransduction mediates hereditary hemorrhagic telangiectasia. *J Cell Biol* **214**, 807-816, doi:10.1083/jcb.201603106 (2016).

6 Deng, H. *et al.* Activation of Smad2/3 signaling by low fluid shear stress mediates artery inward remodeling. *Proc Natl Acad Sci U S A* **118**, doi:10.1073/pnas.2105339118 (2021).

7 Jin, Y. *et al.* Endoglin prevents vascular malformation by regulating flow-induced cell migration and specification through VEGFR2 signalling. *Nature Cell Biology* **19**, 639-+, doi:10.1038/ncb3534 (2017).

8 Ola, R. *et al.* SMAD4 Prevents Flow Induced Arteriovenous Malformations by Inhibiting Casein Kinase 2. *Circulation* **138**, 2379-2394, doi:10.1161/CIRCULATIONAHA.118.033842 (2018).

9 Johnson, D. W. *et al.* Mutations in the activin receptor-like kinase 1 gene in hereditary haemorrhagic telangiectasia type 2. *Nat Genet* **13**, 189-195, doi:10.1038/ng0696-189 (1996).

10 McAllister, K. A. *et al.* Endoglin, a TGF-beta binding protein of endothelial cells, is the gene for hereditary haemorrhagic telangiectasia type 1. *Nat Genet* **8**, 345-351, doi:10.1038/ng1294-345 (1994).

11 Teekakirikul, P. *et al.* Thoracic aortic disease in two patients with juvenile polyposis syndrome and SMAD4 mutations. *Am J Med Genet A* **161A**, 185-191, doi:10.1002/ajmg.a.35659 (2013).

12 Iriarte, A. *et al.* PI3K (Phosphatidylinositol 3-Kinase) Activation and Endothelial Cell Proliferation in Patients with Hemorrhagic Hereditary Telangiectasia Type 1. *Cells* **8**, doi:ARTN 97110.3390/cells8090971 (2019).

13 Ola, R. *et al.* PI3 kinase inhibition improves vascular malformations in mouse models of hereditary haemorrhagic telangiectasia. *Nat Commun* **7**, 13650, doi:10.1038/ncomms13650 (2016).

14 Dimmeler, S., Assmus, B., Hermann, C., Haendeler, J. & Zeiher, A. M. Fluid shear stress stimulates phosphorylation of Akt in human endothelial cells: involvement in suppression of apoptosis. *Circ Res* **83**, 334-341, doi:10.1161/01.res.83.3.334 (1998).

15 Park, H. *et al.* Defective Flow-Migration Coupling Causes Arteriovenous Malformations in Hereditary Hemorrhagic Telangiectasia. *Circulation* **144**, 805-822, doi:10.1161/CIRCULATIONAHA.120.053047 (2021).

16 Akimoto, S., Mitsumata, M., Sasaguri, T. & Yoshida, Y. Laminar shear stress inhibits vascular endothelial cell proliferation by inducing cyclin-dependent kinase inhibitor p21(Sdi1/Cip1/Waf1). *Circ Res* **86**, 185-190, doi:10.1161/01.res.86.2.185 (2000).
17 Bernabeu, M. O. *et al.* Computer simulations reveal complex distribution of haemodynamic forces in a mouse retina model of angiogenesis. *Journal of the Royal Society Interface* **11**, doi:ARTN 20140543 10.1098/rsif.2014.0543 (2014).
18 Nagaoka, T. & Yoshida, A. Noninvasive evaluation of wall shear stress on retinal microcirculation in humans. *Investigative Ophthalmology & Visual Science* **47**, 1113-1119, doi:10.1167/iovs.05-0218 (2006).
19 Hamik, A. *et al.* Kruppel-like factor 4 regulates endothelial inflammation. *J Biol Chem* **282**, 13769-13779, doi:10.1074/jbc.M700078200 (2007).
20 Peacock, H. M. *et al.* Impaired SMAD1/5 Mechanotransduction and Cx37 (Connexin37) Expression Enable Pathological Vessel Enlargement and Shunting. *Arteriosclerosis Thrombosis and Vascular Biology* **40**, E87-E104, doi:10.1161/Atvbaha.119.313122 (2020).
21 Boon, R. A. *et al.* KLF2-induced actin shear fibers control both alignment to flow and JNK signaling in vascular endothelium. *Blood* **115**, 2533-2542, doi:10.1182/blood-2009-06-228726 (2010).
22 Coon, B. G. *et al.* Intramembrane binding of VE-cadherin to VEGFR2 and VEGFR3 assembles the endothelial mechanosensory complex. *Journal of Cell Biology* **208**, 975-986, doi:10.1083/jcb.201408103 (2015).
23 Tzima, E. *et al.* A mechanosensory complex that mediates the endothelial cell response to fluid shear stress. *Nature* **437**, 426-431, doi:10.1038/nature03952 (2005).
24 Fang, J. S. *et al.* Shear-induced Notch-Cx37-p27 axis arrests endothelial cell cycle to enable arterial specification (vol 8, 2017). *Nature Communications* **9**, doi:ARTN 720 10.1038/s41467-018-03076-4 (2018).
25 Mahmoud, M. *et al.* Pathogenesis of Arteriovenous Malformations in the Absence of Endoglin. *Circulation Research* **106**, 1425-U1270, doi:10.1161/Circresaha.109.211037 (2010).
26 Franco, C. A. *et al.* Non-canonical Wnt signalling modulates the endothelial shear stress flow sensor in vascular remodelling. *Elife* **5**, e07727, doi:10.7554/eLife.07727 (2016).
27 Limaye, N. *et al.* Somatic Activating PIK3CA Mutations Cause Venous Malformation. *Am J Hum Genet* **97**, 914-921, doi:10.1016/j.ajhg.2015.11.011 (2015).
28 Ren, A. A. *et al.* PIK3CA and CCM mutations fuel cavernomas through a cancer-like mechanism. *Nature* **594**, 271-276, doi:10.1038/s41586-021-03562-8 (2021).
29 Jin, Y. *et al.* Endoglin prevents vascular malformation by regulating flow-induced cell migration and specification through VEGFR2 signalling. *Nat Cell Biol* **19**, 639-652, doi:10.1038/ncb3534 (2017).
30 Sugden, W. W. *et al.* Endoglin controls blood vessel diameter through endothelial cell shape changes in response to haemodynamic cues. *Nat Cell Biol* **19**, 653-665, doi:10.1038/ncb3528 (2017).
31 Lee, H. W. *et al.* Role of Venous Endothelial Cells in Developmental and Pathologic Angiogenesis. *Circulation* **144**, 1308-1322, doi:10.1161/CIRCULATIONAHA.121.054071 (2021).

FIGURE 1

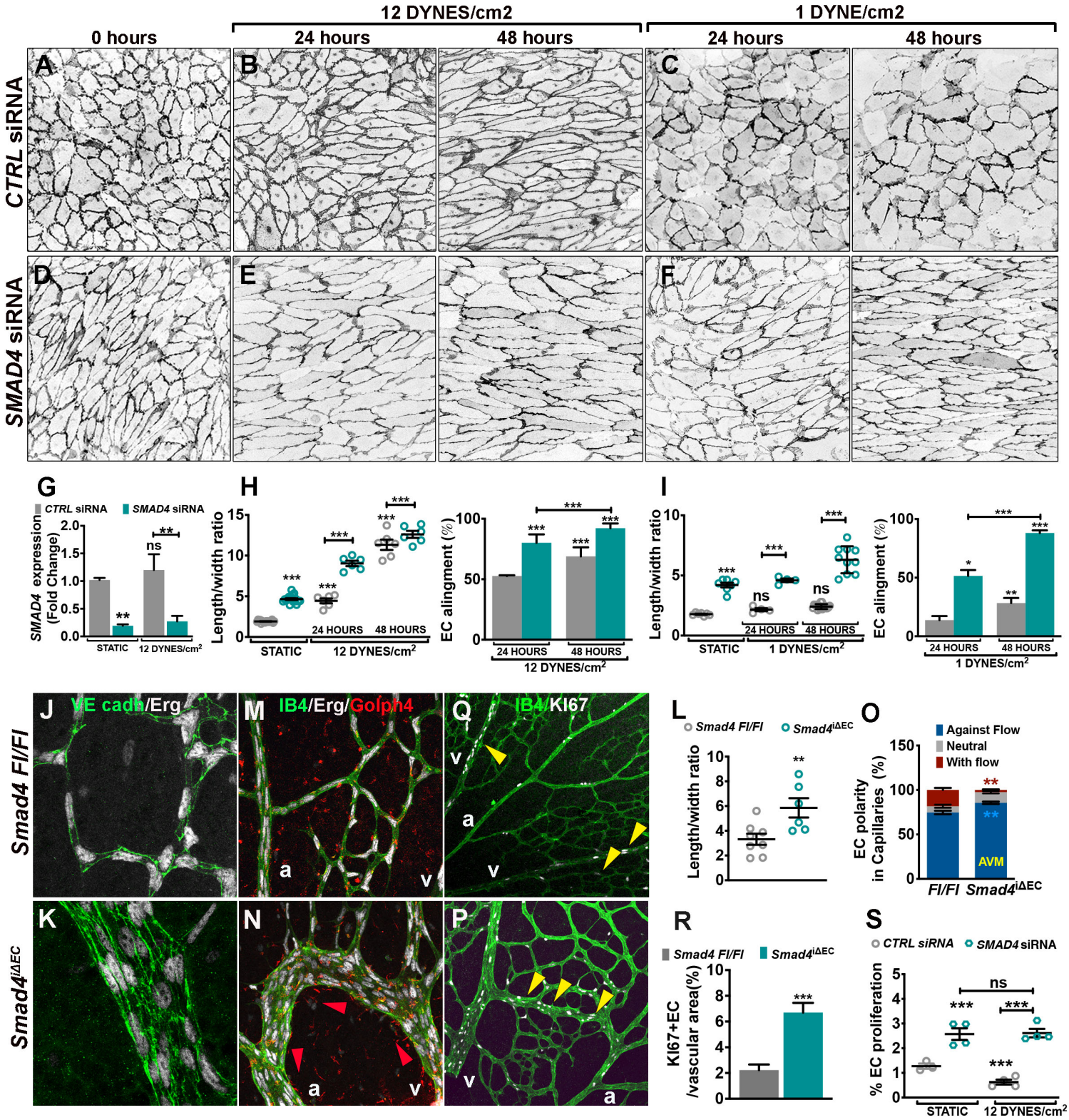
12 DYNES/cm2
1 DYNE/cm2
0 hours
24 hours
48 hours
24 hours
48 hours
CTRL siRNA
SMAD4 siRNA
A
B
C
D
E
F
G
CTRL siRNA
SMAD4 siRNA
SMAD4 expression (Fold Change)
ns
STATIC
12 DYNES/cm2
H
Length/width ratio
24 HOURS
48 HOURS
STATIC
12 DYNES/cm2
EC alingment (%)
24 HOURS
48 HOURS
12 DYNES/cm2
I
Length/width ratio
STATIC
1 DYNES/cm2
EC alingment (%)
1 DYNES/cm2
J
VE cadh/Erg
M
IB4/Erg/Golph4
Q
IB4/KI67
Smad4 Fl/Fl
K
N
P
Smad4iΔEC
L
Smad4 Fl/Fl
Smad4iΔEC
Length/width ratio
O
Against Flow
Neutral
With flow
EC polarity in Capillaries (%)
AVM
Fl/Fl
Smad4iΔEC
R
Smad4 Fl/Fl
Smad4iΔEC
KI67+EC /vascular area(%)
S
CTRL siRNA
SMAD4 siRNA
% EC proliferation
ns
STATIC
12 DYNES/cm2

FIGURE 2

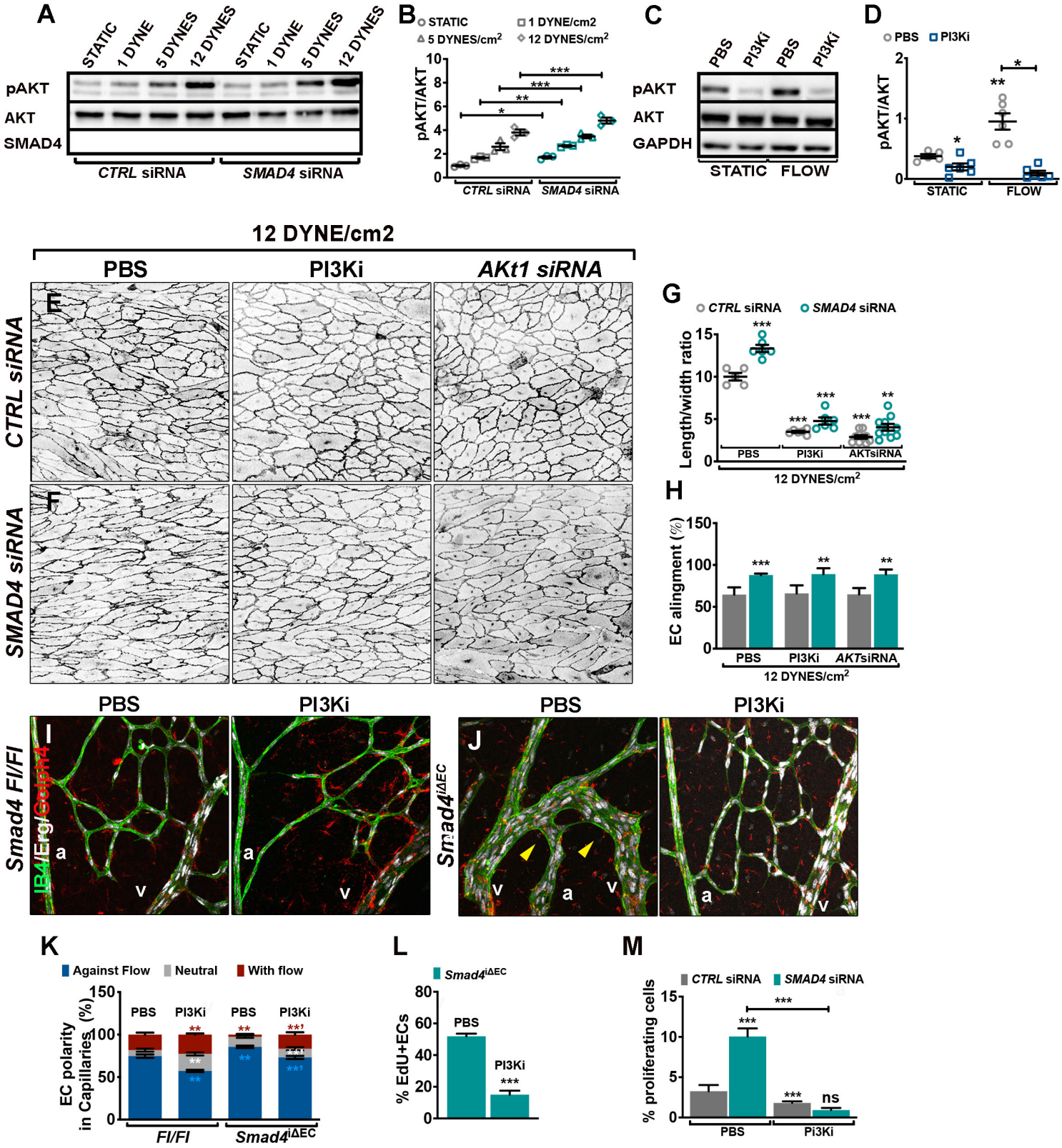
A
STATIC
1 DYNE
5 DYNES
12 DYNES
pAKT
AKT
SMAD4
CTRL siRNA
SMAD4 siRNA
B
STATIC
1 DYNE/cm2
5 DYNES/cm2
12 DYNES/cm2
pAKT/AKT
CTRL siRNA
SMAD4 siRNA
C
PBS
PI3Ki
pAKT
AKT
GAPDH
STATIC
FLOW
D
PBS
PI3Ki
pAKT/AKT
STATIC
FLOW
12 DYNE/cm2
PBS
PI3Ki
AKt1 siRNA
CTRL siRNA
SMAD4 siRNA
E
F
G
CTRL siRNA
SMAD4 siRNA
Length/width ratio
PBS
PI3Ki
AKTsiRNA
12 DYNES/cm2
H
EC alingment (%)
PBS
PI3Ki
AKTsiRNA
12 DYNES/cm2
Smad4 Fl/Fl
PBS
PI3Ki
I
IB4/Erg/Golph4
a
v
J
Smad4iΔEC
K
Against Flow
Neutral
With flow
EC polarity in Capillaries (%)
PBS
PI3Ki
Fl/Fl
Smad4iΔEC
L
Smad4iΔEC
% EdU+ECs
PBS
PI3Ki
M
CTRL siRNA
SMAD4 siRNA
% proliferating cells
PBS
Pi3Ki
ns

FIGURE 3

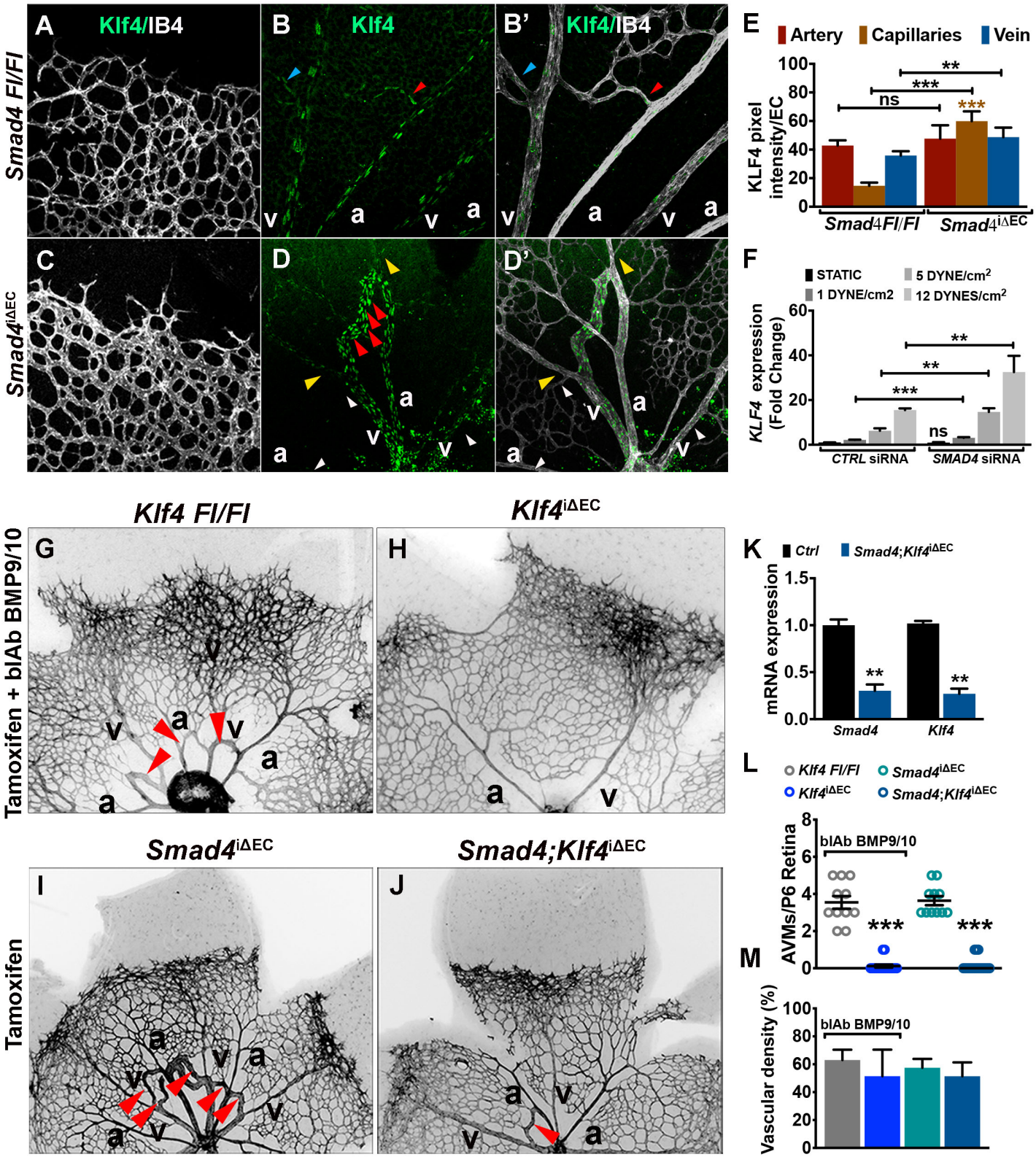
A
Klf4/IB4
B
Klf4
B'
Klf4/IB4
Smad4 Fl/Fl
C
D
D'
Smad4iΔEC
E
Artery
Capillaries
Vein
KLF4 pixel intensity/EC
ns
***
**
Smad4Fl/Fl
Smad4iΔEC
F
STATIC
5 DYNE/cm2
1 DYNE/cm2
12 DYNES/cm2
KLF4 expression (Fold Change)
CTRL siRNA
SMAD4 siRNA
Klf4 Fl/Fl
Klf4iΔEC
Tamoxifen + bIAb BMP9/10
G
H
K
Ctrl
Smad4;Klf4iΔEC
mRNA expression
Smad4
Klf4
L
Klf4 Fl/Fl
Klf4iΔEC
Smad4iΔEC
Smad4;Klf4iΔEC
AVMs/P6 Retina
bIAb BMP9/10
Smad4iΔEC
Smad4;Klf4iΔEC
Tamoxifen
I
J
M
Vascular density (%)
bIAb BMP9/10

FIGURE 4

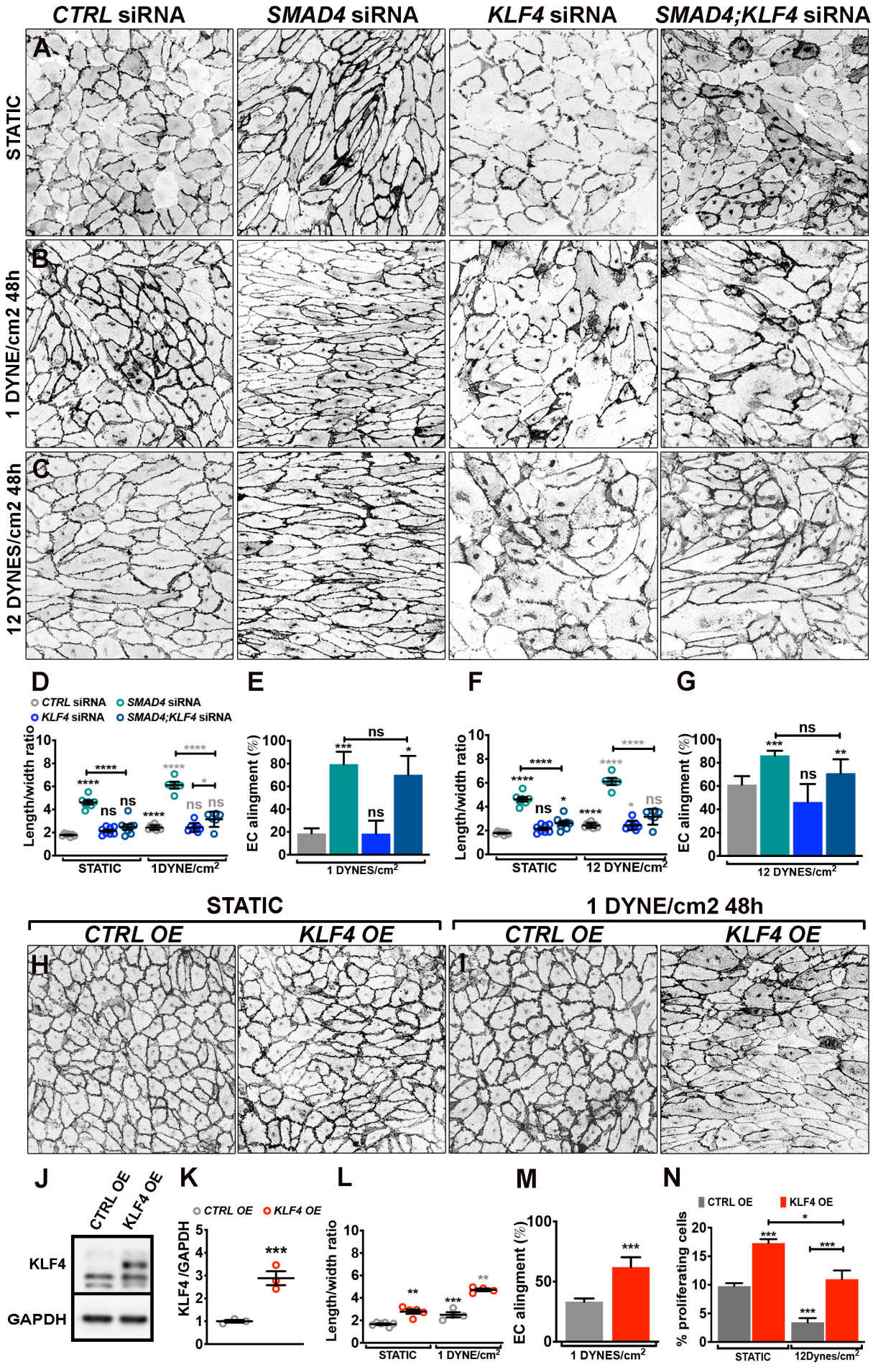
CTRL siRNA
SMAD4 siRNA
KLF4 siRNA
SMAD4;KLF4 siRNA
A
B
C
STATIC
1 DYNE/cm2 48h
12 DYNES/cm2 48h
D
E
F
G
CTRL siRNA
SMAD4 siRNA
KLF4 siRNA
SMAD4;KLF4 siRNA
Length/width ratio
EC alingment (%)
STATIC
1DYNE/cm2
1 DYNES/cm2
12 DYNE/cm2
12 DYNES/cm2
ns
STATIC
1 DYNE/cm2 48h
CTRL OE
KLF4 OE
H
I
J
K
L
M
N
KLF4
GAPDH
KLF4 /GAPDH
Length/width ratio
EC alingment (%)
% proliferating cells
STATIC
1 DYNE/cm2
1 DYNES/cm2
12Dynes/cm2

FIGURE 5

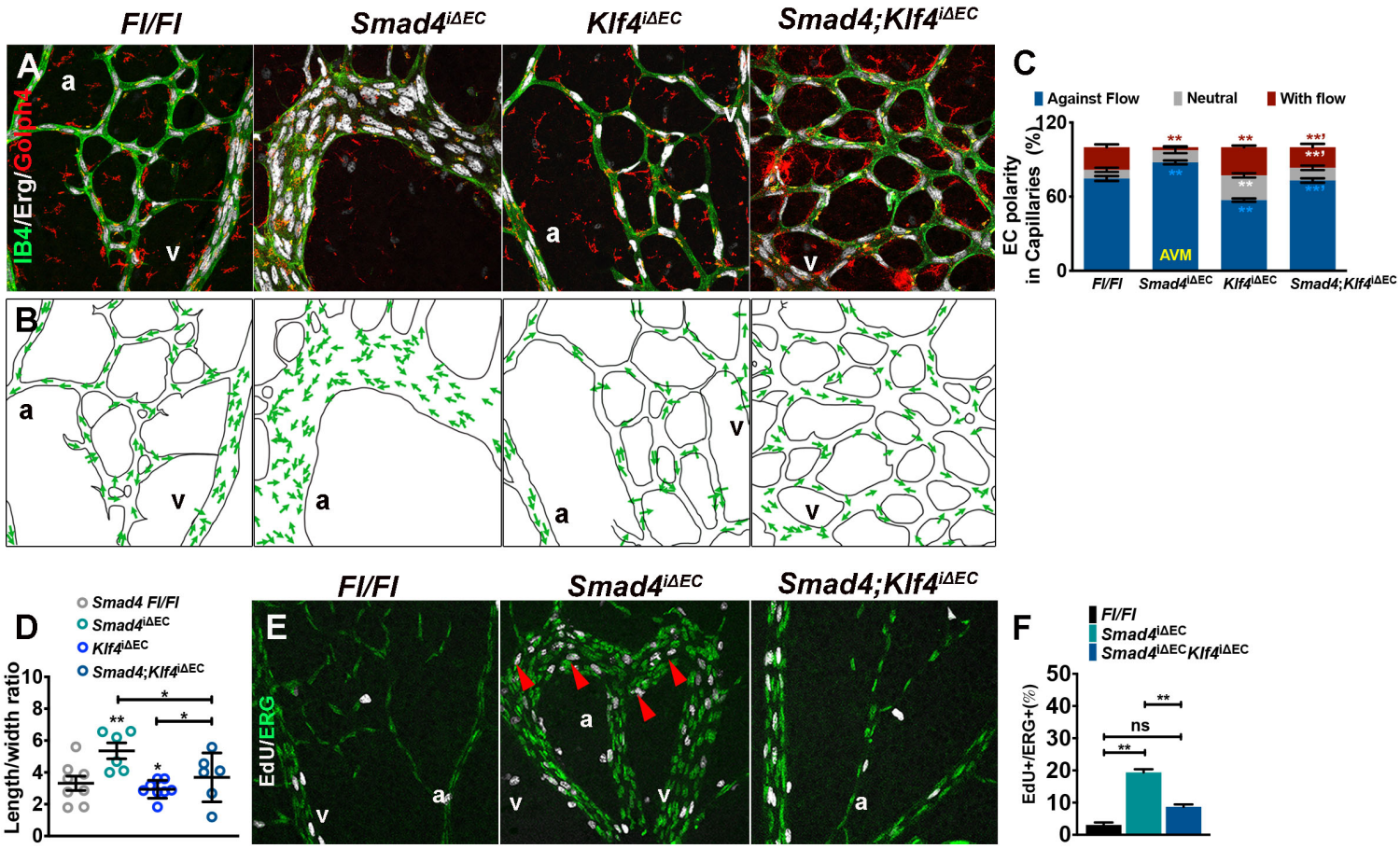
Fl/Fl
Smad4iΔEC
Klf4iΔEC
Smad4;Klf4iΔEC
A
IB4/Erg/Golph4
a
v
B
C
Against Flow
Neutral
With flow
EC polarity in Capillaries (%)
120
60
0
AVM
D
Smad4 Fl/Fl
Smad4iΔEC
Klf4iΔEC
Smad4;Klf4iΔEC
Length/width ratio
10
8
6
4
2
0
E
EdU/ERG
F
Fl/Fl
Smad4iΔEC
Smad4iΔECKlf4iΔEC
EdU+/ERG+(%)
50
40
30
20
10
0
ns

FIGURE 6

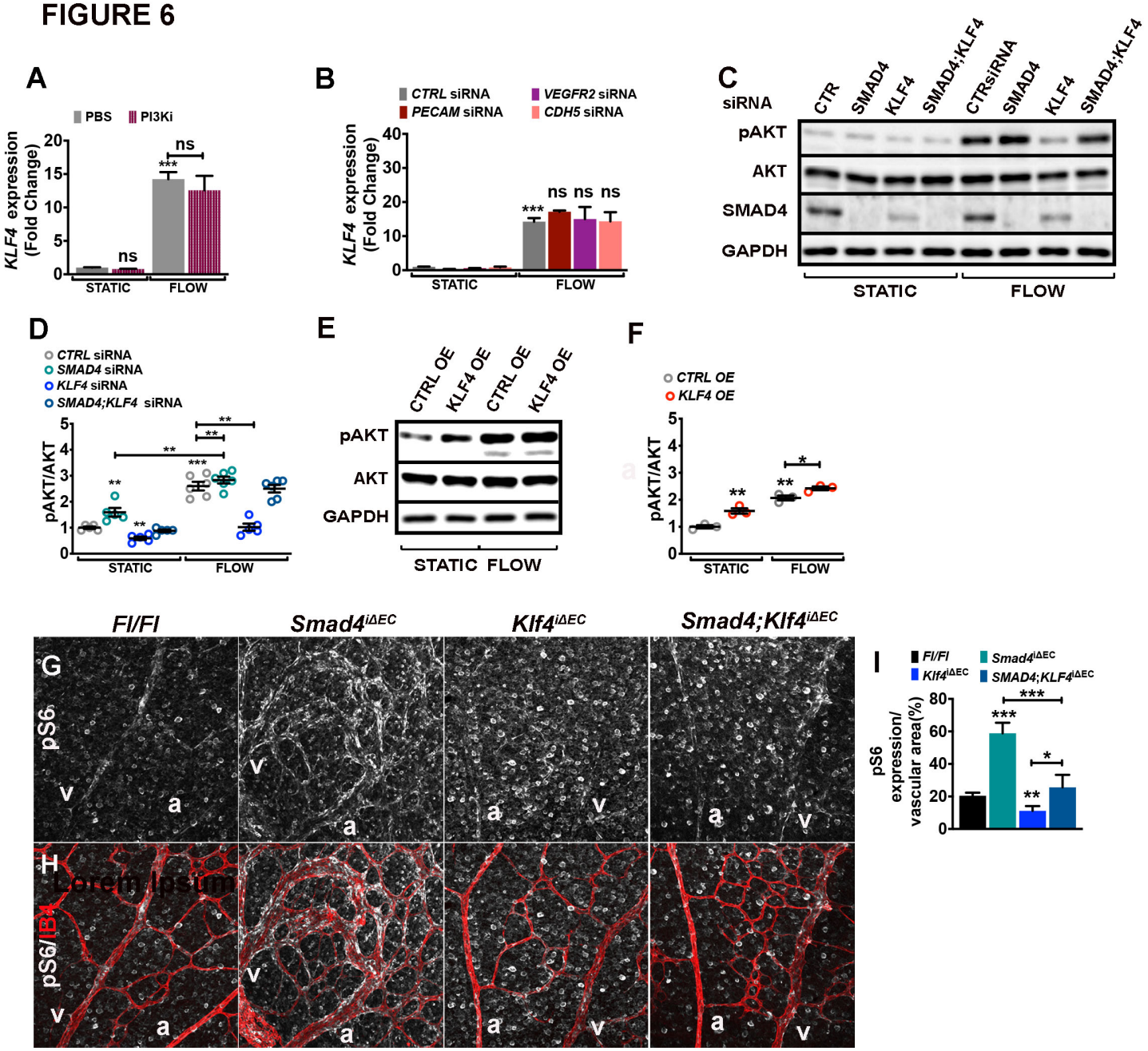
A
PBS
PI3Ki
KLF4 expression (Fold Change)
ns
***
ns
STATIC
FLOW
B
CTRL siRNA
PECAM siRNA
VEGFR2 siRNA
CDH5 siRNA
KLF4 expression (Fold Change)
***
ns ns ns
STATIC
FLOW
C
siRNA
CTR
SMAD4
KLF4
SMAD4;KLF4
CTRsiRNA
SMAD4
KLF4
SMAD4;KLF4
pAKT
AKT
SMAD4
GAPDH
STATIC
FLOW
D
CTRL siRNA
SMAD4 siRNA
KLF4 siRNA
SMAD4;KLF4 siRNA
pAKT/AKT
STATIC
FLOW
E
CTRL OE
KLF4 OE
CTRL OE
KLF4 OE
pAKT
AKT
GAPDH
STATIC FLOW
F
CTRL OE
KLF4 OE
pAKT/AKT
STATIC
FLOW
Fl/Fl
Smad4iΔEC
Klf4iΔEC
Smad4;Klf4iΔEC
G
pS6
v
a
H
pS6/IB4
Lorem Ipsum
I
Fl/Fl
Smad4iΔEC
Klf4iΔEC
SMAD4;KLF4iΔEC
pS6 expression/ vascular area(%)

FIGURE 7

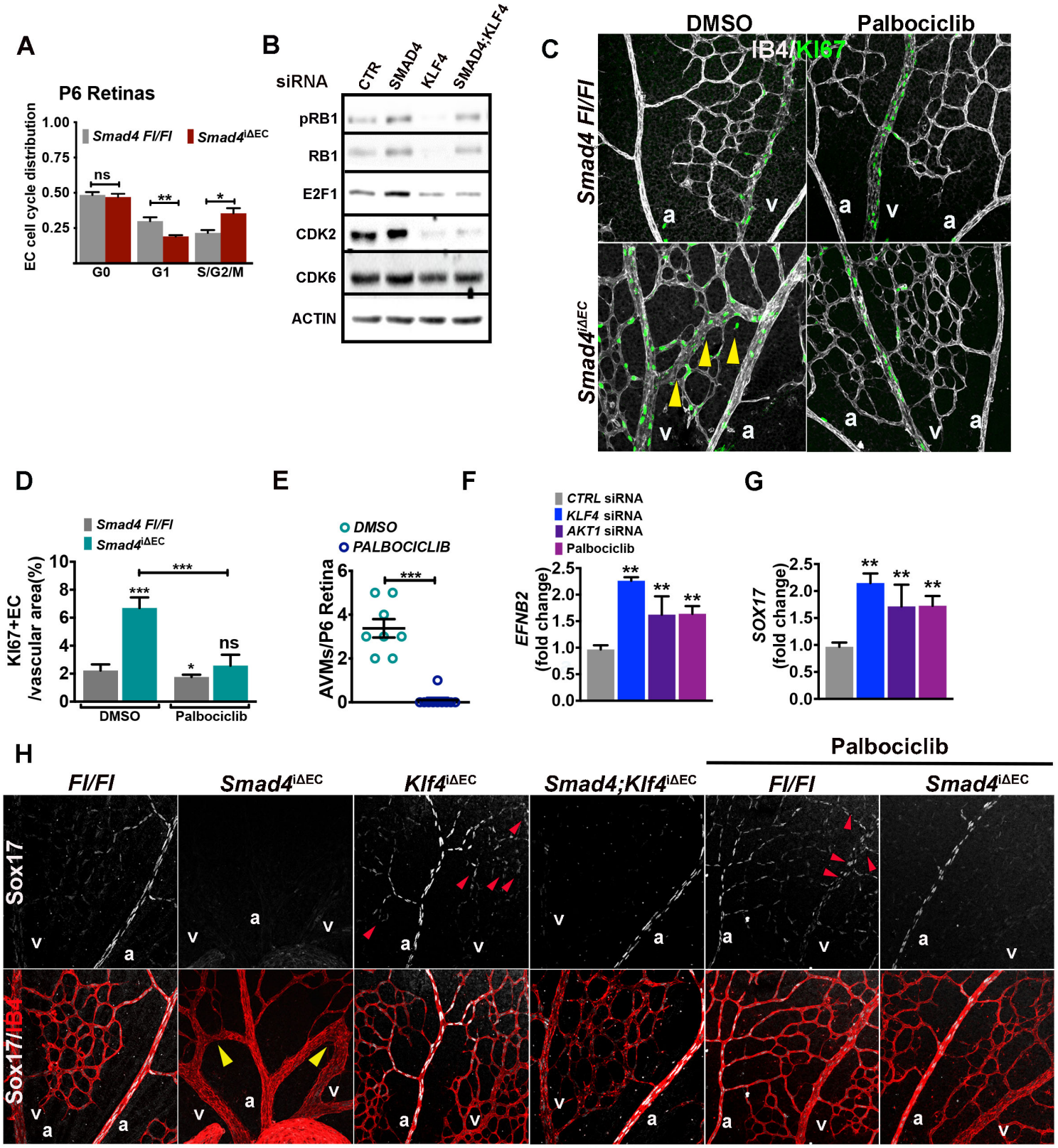
A
P6 Retinas
EC cell cycle distribution
Smad4 Fl/Fl
Smad4iΔEC
ns
**
*
G0
G1
S/G2/M
B
siRNA
CTR
SMAD4
KLF4
SMAD4;KLF4
pRB1
RB1
E2F1
CDK2
CDK6
ACTIN
C
DMSO
Palbociclib
IB4/KI67
Smad4 Fl/Fl
Smad4iΔEC
a
v
D
Smad4 Fl/Fl
Smad4iΔEC
KI67+EC /vascular area(%)
***
ns
DMSO
Palbociclib
E
DMSO
PALBOCICLIB
AVMs/P6 Retina
F
CTRL siRNA
KLF4 siRNA
AKT1 siRNA
Palbociclib
EFNB2 (fold change)
G
SOX17 (fold change)
H
Palbociclib
Fl/Fl
Smad4iΔEC
Klf4iΔEC
Smad4;Klf4iΔEC
Sox17
Sox17/IB4